Decreased Androgen Receptor Levels and Receptor Function in Breast Cancer Contribute to the Failure of Response to Medroxyprogesterone Acetate

Grant Buchanan,[1] Stephen N. Birrell,[1] Amelia A. Peters,[1] Tina Bianco-Miotto,[1] Katrina Ramsay,[1] Elisa J. Cops,[1] Miao Yang,[1] Jonathan M. Harris,[2] Henry A. Simila,[2] Nicole L. Moore,[3] Jacqueline M. Bentel,[3] Carmella Ricciardelli,[1] David J. Horsfall,[1] Lisa M. Butler,[1] and Wayne D. Tilley[1]

[1]Dame Roma Mitchell Cancer Research Laboratories, University of Adelaide/Hanson Institute, Adelaide, South Australia, Australia; [2]Queensland University of Technology, Brisbane, Queensland, Australia; and [3]Department of Pathology, Royal Perth Hospital, Perth, Western Australia, Australia

Abstract

Previously, we reported that androgen receptor (AR), but not estrogen receptor (ER) or progesterone receptor (PR), is predictive of response to the synthetic progestin, medroxyprogesterone acetate (MPA), in a cohort of 83 patients with metastatic breast cancer. To further investigate the role of AR in determining response to MPA in this cohort, we analyzed AR levels by immunohistochemistry with two discrete antisera directed at either the NH_2 or the COOH termini of the receptor. Compared with tumors that responded to MPA (n = 31), there was a significant decrease in the intensity and extent of AR immunoreactivity with both AR antisera in tumors from nonresponders (n = 52). Whereas only a single AR immunostaining pattern was detected in responders to MPA, reflecting concordance of immunoreactivity with the two AR antisera, tumors from nonresponders exhibited four distinct AR immunostaining patterns: (a) concordance with the two antibodies (31%), (b) staining only with the COOH-terminal antibody (33%), (c) staining only with the NH_2-terminal antibody (22%), or (d) no immunoreactivity with either NH_2- or COOH-terminal antibody (14%). DNA sequencing and functional analysis identified inactivating missense gene mutations in the ligand-binding domain of the AR in tumors from two of nine nonresponders positive with the NH_2-terminal AR antisera but negative for COOH-terminal immunoreactivity and lacking specific, high-affinity dihydrotestosterone binding in tumor cytosol fractions. Tumors with more AR than the median level (37 fmol/mg protein) had significantly lower levels of PR (30 fmol/mg protein) than tumors with low AR (PR; 127 fmol/mg protein) despite comparable levels of ER. Ligand-dependent activation of the AR in human T47D and MCF-7 breast cancer cells resulted in inhibition of estradiol-stimulated cell proliferation and a reduction in the capacity of the ER to induce expression of the PR. These effects could be reversed using a specific AR antisense oligonucleotide. Increasing the ratio of AR to ER resulted in a greater androgen-dependent inhibition of ER function. Collectively, these data suggest that reduced levels of AR or impaired AR function contribute to the failure of MPA therapy potentially due to abrogation of the inhibitory effect of AR on ER signaling. (Cancer Res 2005; 65(18): 8487-96)

Introduction

Although androgen signaling has been extensively studied in the prostate (1), there is emerging evidence that androgens have inhibitory effects on the growth of breast epithelial cells and play a protective role in the pathogenesis of breast cancer (2–5). The androgen receptor (AR) is expressed in ~70% to 90% of primary breast tumors, a frequency comparable with or higher than that reported for either the estrogen receptor (ER; 70-80%) or the progesterone receptor (PR; 50-70%; refs. 6, 7). Importantly, comprehensive microarray analysis recently determined that mammary tumor cells can be divided into three groups based on steroid receptor activity: luminal (ER+, AR+), basal (ER−, AR−), and apocrine (ER−, AR+; ref. 8). In addition, several case-control studies have identified a relationship between breast cancer risk and length of the polymorphic CAG repeat in exon 1 of the *AR* gene (9), an established modulator of AR function (10, 11).

Androgens (e.g., fluoxymesterone) have a comparable efficacy with that of current hormonal treatments for advanced breast cancer, but their use as primary therapeutic agents declined with the advent of tamoxifen (12, 13). Nevertheless, the potential for androgens to counterbalance positive growth stimuli in the breast has been pursued in recent *in vivo* studies in rhesus monkeys, where blocking the action of endogenous androgens resulted in a 2-fold increase in the proliferation of mammary epithelial cells (14). Conversely, low doses of testosterone completely inhibited estrogen-mediated mammary cell proliferation in ovariectomized animals (14). Similarly, in culture, androgens predominantly exhibit an inhibitory effect on AR-positive breast cancer cell lines (2, 15, 16).

The synthetic progestin, medroxyprogesterone acetate (MPA), was used frequently until the early 1990s as a second-line hormonal therapy for metastatic breast cancer (17). Although the use of MPA declined following the advent of tamoxifen and aromatase inhibitors, recently, there has been renewed interest in alternative hormonal treatments, including MPA, for use both in early disease and in the advanced setting when conventional therapies fail (18–20). Whereas MPA was designed to bind with high affinity to the PR, the androgenic side effects observed in women taking MPA suggested that the AR may contribute to its activity *in vivo*. This hypothesis is supported by the high binding affinity of MPA to the AR

Note: N. Moore is currently at the Department of Molecular and Cellular Biology, Baylor College of Medicine, Houston, Texas.

Requests for reprints: Wayne D. Tilley, Dame Roma Mitchell Cancer Research Laboratories, University of Adelaide/Hanson Institute, P.O. Box 14, Rundle Mall, Adelaide, South Australia 5000, Australia. Phone: 61-8-8222-3225; Fax: 61-8-8222-3217; E-mail: wayne.tilley@imvs.sa.gov.au.

doi:10.1158/0008-5472.CAN-04-3077

(21) and clinical studies showing the response of breast tumors to high-dose MPA therapy is dependent on expression of the AR but not the PR (22, 23). A recent report that the length of the AR CAG repeat is correlated with breast density in women receiving combined hormone replacement therapy (24) provides additional evidence that AR is a determinant of the effects of MPA in the breast. Furthermore, MPA inhibits the proliferation of AR-positive but not AR-negative breast cancer cell lines, and this inhibition can be reversed by cotreatment with specific AR antagonists (21, 25).

We reported previously that the response of breast cancers to MPA in a cohort 83 women who failed tamoxifen therapy was related to the AR level by radioligand binding in the primary tumor but not to ER or PR. However, 33% of tumors that failed to respond to MPA had detectable AR by radioligand binding. Therefore, in the current study, we used an immunohistochemistry strategy with discrete antisera directed against the NH_2- and COOH-termini of the AR, employed previously in the identification of AR variants in prostate cancer (26, 27), to examine whether failure of MPA therapy is associated with altered AR levels and/or the presence of structural variants of the AR.

Materials and Methods

Tissues and clinical data. This study consisted of a total of 161 postmenopausal women treated for early-stage breast cancer (International Union Against Cancer stage IIa or IIb) between 1984 and 1987 at the Surgical Oncology Unit, Department of Surgery, Flinders Medical Centre (South Australia, Australia). Patients received either a partial (33%) or a total (67%) mastectomy with axillary clearance, and 141 were treated postoperatively with indefinite adjuvant tamoxifen [one 20 mg tablet daily of Nolvadex-D, ICI Pharmaceuticals Pty Ltd., Australia; median (range) duration, 68 (6-110) months]. Of the 89 patients who relapsed on tamoxifen, 83 were subsequently treated with MPA (one 500 mg tablet daily of Farlutal, Farmitalia Pty Ltd., Australia). Clinical examination was done every 3 months, and nuclear bone scans, chest X-rays, and hematologic and biochemical blood analyses were done initially at 3 months and then six monthly or more frequently if clinically indicated. After relapse on MPA, patients were clinically evaluated at least every 3 months until death. Response to MPA was defined by complete disappearance of all known disease, a $\geq$50% decrease in tumor size below baseline using the sum of the product of perpendicular diameters for bidimensional lesions, or a $\geq$30% decrease in tumor size from baseline using the sum of the largest diameter for unidimensional lesions. Nonresponders to MPA were defined by stable (no change in lesion size) or progressive (appearance of new lesions or a >25% increase in bidimensional lesions) disease. The cohort of 26 prostate samples is described elsewhere (27).

Radioligand binding. Breast cancer specimens were obtained on ice from theatre immediately after excision and tumor tissue was separated from macroscopically normal tissue. AR, ER, and PR status was determined by the South Australian State Diagnostic Hormone Receptor Laboratory at Flinders Medical Centre. Tissues were homogenized in cytosol buffer [10 mmol/L Tris, 1.5 mmol/L sodium molybdate, 10% glycerol (pH 7.4), 1 mmol/L DTT] and soluble cytosol fractions were prepared by ultracentrifugation. Five incubating concentrations (in duplicate), ranging from 0.02 to 5.0 nmol/L of the specific titrated ligand, were used to determine total radioligand binding in the cytosol fractions. A parallel series of incubations containing the radioligand in the presence of a 100-fold excess of unlabeled ligand were used to estimate nonspecific binding. In assays for AR, a 500-fold excess of triamcinolone acetonide was incorporated into both total and nonspecific binding incubations to block [^{3}H]R1881 binding to PR. Bound and free hormone were separated using dextran-coated charcoal, and total and nonspecific binding was measured by scintillation counting. Data were analyzed by Scatchard plot and least-squares regression analysis. The specific radioligands used were [^{3}H]R1881 (methyltrienolone; 80 Ci/mmol; New England Nuclear, Sydney, New South Wales, Australia) for AR, estradiol (101 Ci/mmol; Amersham Biosciences, Castle Hill, NSW, Australia) for ER, and [^{3}H]R5020 (83 Ci/mmol; New England Nuclear) for PR.

Immunohistochemical analysis of androgen receptor. Formalin-fixed, paraffin-embedded breast tumor specimens for the 83 women who received MPA were obtained from the Department of Anatomical Pathology, Flinders Medical Centre, with approval of the Committee on Clinical Investigations. Immunohistochemical staining for AR was done on serial 4 μm sections using the AR NH_2-terminal U402 and COOH-terminal R489 antisera directed at the NH_2-terminal 21 and COOH-terminal 20 amino acids of the wild-type AR (wtAR), respectively (28). Visualization of AR was achieved with a standard immunoperoxidase reaction using biotinylated anti-rabbit antibody (1:400, DAKO Corp., Carpinteria, CA), streptavidin-horseradish peroxidase (HRP) complex (1:500, DAKO), and diaminobenzidine tetrahydrochloride to yield an insoluble brown deposit. AR immunoreactivity was assessed in tumor foci at a magnification of ×400. Immunostaining was quantified using color video image analysis (VIA) as described previously (26). Video image measurements included the total nuclear area of tissue examined (i.e., positively and negatively stained nuclear area in pixel units) and the diaminobenzidine tetrahydrochloride–stained area (i.e., positively stained nuclear area in pixel units). These values were used to derive percent AR-positive nuclear area and mean intensity of AR immunoreactivity. VIA data represent image analysis done for at least 20 randomly selected fields in each sample.

Single-strand conformational polymorphism analysis and DNA sequencing. Genomic DNA was isolated from 25 μm sections of breast cancer tissue as described previously (27). The coding sequence of the AR ligand-binding domains (LBD) was amplified by PCR using sets of overlapping primers and a 1:16 mixture of *pfu* and *taq* polymerases and analyzed by single-strand conformational polymorphism (SSCP) analysis on nondenaturing polyacrylamide gels (6% polyacrylamide, 5% glycerol gel; either 10°C or 28°C for 16 hours) according to previously published methods (27). Fragments of AR exhibiting a consistent mobility shift in at least two independent SSCP analyses for a single tumor sample were amplified in independent reactions and cloned into the pCRII TA vector (Invitrogen, San Diego, CA). Sequencing was done using the Sequenase 7-deaza-dGTP DNA Sequencing kit (Amersham) and a 373A PE Biosystems automated DNA sequencer (Applied Biosystems, Foster City, CA). Mutations were scored if they were confirmed by sequencing of both sense and antisense strands in two or more independent clones. Based on a range (10-3,000 copies) of template DNA and the documented error rate of a 1:16 mixture of *pfu* and *taq* polymerases (5.6×10^{-6} per base; ref. 29), <2.5% of final PCR amplicons of 250 bp long (the upper limit in this study) were predicted to contain misincorporation errors, which is below the threshold for detection by SSCP analysis.

Cell culture. COS-1, CV-1, LNCaP, T47D, and MDA-MB-231 cells were obtained from the American Type Culture Collection (Manassas, VA) and maintained in RPMI 1640 supplemented with 5% fetal bovine serum (FBS). The PC-3^{AR-} subline described elsewhere (30) was also used in this study.

Construction of androgen receptor variant expression plasmids. Base substitutions required to generate AR variants were introduced into an expression vector containing the complete human *AR* gene coding sequence (pCMV-AR; ref. 31) by PCR-based megaprimer *in vitro* mutagenesis as described previously (10, 30). The presence of the required base substitutions and integrity of AR variant plasmid constructs was confirmed by DNA sequencing.

Cell proliferation and viability. T47D and MCF-7 cells were seeded into 24-well tissue culture plates at 50,000 cells per well in phenol red–free RPMI 1640 supplemented with 5% dextran-coated charcoal-stripped FCS. Two days after seeding, cells were washed and treated for 6 days with medium containing the appropriate steroids (replaced each 3 days). Cells were trypsinized and counted using a hemocytometer at day 6, with viability determined using trypan blue exclusion. To knockdown endogenous levels of AR, cells were allowed to adhere for 2 days and then transfected for 5 hours with 580 ng/well of either the specific AR antisense oligonucleotide (5′-CTGCACTTCCATCCT-3′; ref. 2) or a scrambled control using Lipofectin (Invitrogen). Cells were subsequently treated and assayed as detailed above.

***In vitro* transactivation assay.** AR and ER transactivation assays were done as described previously (10, 30) in cultured cells (10,000-20,000 cells per well in 96-well plates) cotransfected with 2.5 to 10 ng AR (pCMV-AR; or AR variants) and/or ER (pHEGO) expression vectors and 100 ng of the

appropriate androgen [probasin, ARR3tk-luc; mouse mammary tumor virus (MMTV)-Luc] or estrogen (ERE-tk-luc) luciferase reporter constructs using LipofectAMINE 2000 (Life Technologies, Melbourne, Victoria, Australia) according to the manufacturer's protocol. Luciferase activity was determined using the Luciferase Reporter Gene Assay kit (Promega, Madison, WI) and a plate reading luminometer (Top Count, Packard, Mount Waverley, Australian Capital Territory, Australia) in lysed cells 30 hours after treatment with 0.01 to 1,000 nmol/L steroids and/or specific antagonist in phenol red–free RPMI containing 5% charcoal-stripped FBS. Endogenous ER activity in T47D cells was measured 30 hours after treatment with the appropriate steroids in cells transfected with ERE-tk-luc alone.

Immunoblot analysis. Protein lysates (20 μg) from untransfected LNCaP, T47D, or MCF-7 cells (1×10^6 per 60 mm dish) or COS-1 cells (1×10^6-5×10^6 per 60 mm dish) transfected with 5 μg AR expression vector and grown for 36 hours were electrophoresed on 6% SDS-polyacrylamide gels, transferred to Hybond-C membrane (Amersham), and immunostained using cytokeratin 8 (Sigma, St. Louis, MO), β-actin (Santa Cruz Biotechnology, Santa Cruz, CA), prostate-specific antigen (PSA; DAKO), AR (21), PR (hPRa3 antibody obtained from Dr. Christine Clarke (Department of Medical Oncology, University of Sydney Westmead Hospital, New South Wales, Australia), or ERα (Santa Cruz Biotechnology) antisera. Immunoreactivity was detected using the appropriate HRP-conjugated IgG and visualized using enhanced chemiluminescence (Amersham).

Affinity of dihydrotestosterone and medroxyprogesterone acetate for the androgen receptor and androgen receptor-ligand stability. Affinity of [^{3}H]dihydrotestosterone (DHT; 126 Ci/mmol; Amersham) and

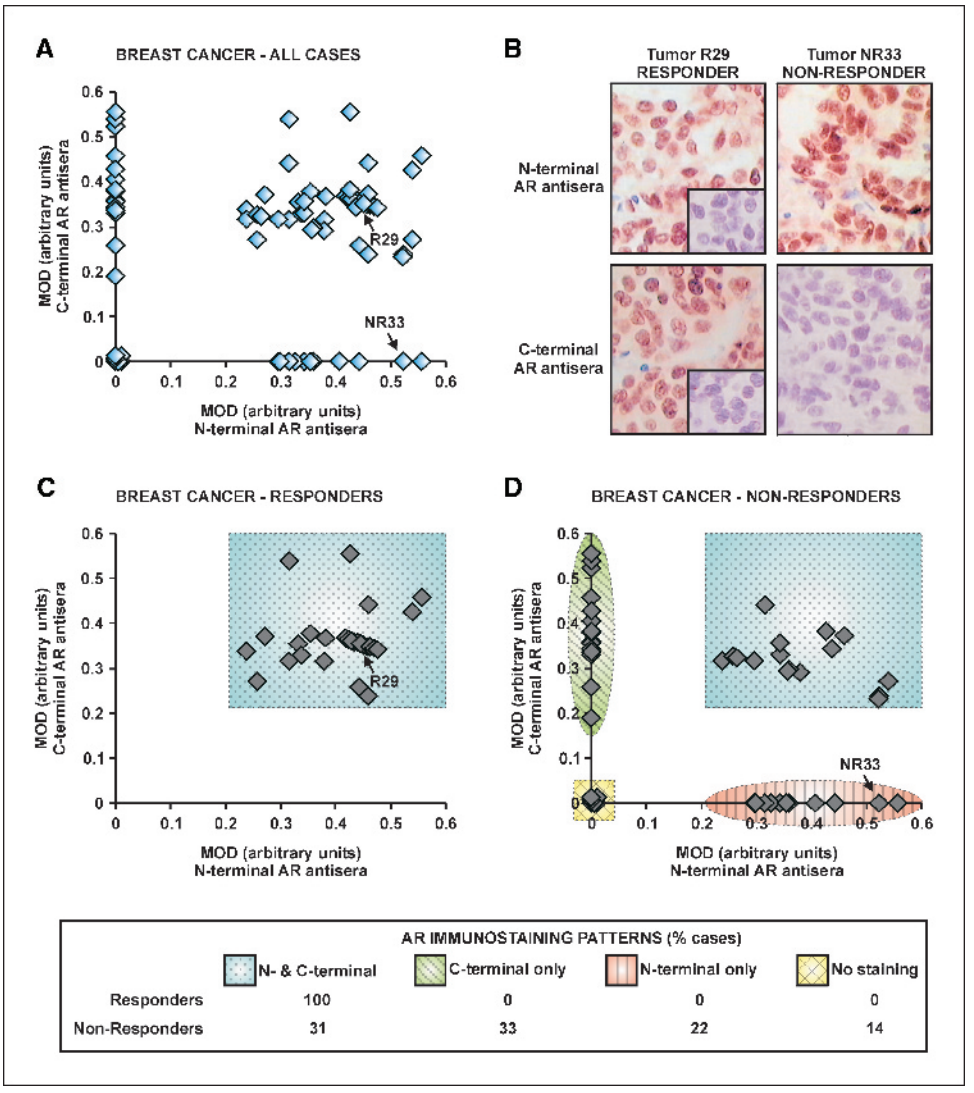

Figure 1. AR immunoreactivity in human breast tumors. *A,* comparison of the mean absorbance (*MOD*; average intensity of AR immunoreactivity) with NH_2- and COOH-terminal AR antisera in 83 human breast tumors from women who received MPA therapy. Data for each antibody were generated using quantitative VIA of at least 20 fields of view chosen at random in each sample. *Arrows,* position of the two examples shown in (*B*). *B,* representative AR immunoreactivity in two breast tumors with the anti–NH_2-terminal (U402) antibody, raised against the NH_2-terminal 21 amino acids, and the anti–COOH-terminal (R489) antibody that was raised against the COOH-terminal 20 amino acids of the receptor. The first tumor shows concordant immunoreactivity with the two antisera in a patient (R29) that responded to MPA treatment. The AR level detected by radioligand binding in this tumor was 221 fmol/mg protein. *Insets,* separate sections of the same tumor that were not incubated with the primary AR antibody. The second tumor, derived from a patient who did not respond to MPA (NR33), stained strongly with the NH_2-terminal but not the COOH-terminal AR antisera. No AR radioligand binding was detected in this tumor. *C,* comparison of mean absorbance with NH_2- and COOH-terminal AR antisera in 32 breast tumors from women who responded to MPA therapy. There was strong AR immunoreactivity with each antisera in all tumors in this group [32 of 32 (100%), *blue-boxed area*]. *D,* comparison of mean absorbance with NH_2- and COOH-terminal AR antisera in 51 breast tumors from women who did not respond to MPA therapy. Tumors could be classified into four distinct groups; (*a*) strong immunoreactivity with both NH_2- and COOH-terminal AR antibodies [16 of 51 (31%), *blue box with dots*], (*b*) strong immunoreactivity with only the AR COOH-terminal antibody [17 of 51 (33%), *green ellipse with stripes on the Y axis*], (*c*) strong immunoreactivity with only the AR NH_2-terminal antibody [11 of 51 (22%), *pink ellipse with vertical lines on the X axis*], and (*d*) no immunoreactivity with either NH_2- or COOH-terminal antibodies [7 of 51 (14%), *cross-hatched yellow box*].

Table 1. AR immunostaining and AR mutational analysis in human breast tumors

Tumor sample	MOD*		%POS†		Mutation‡	
	NH_2 terminal	COOH terminal	NH_2 terminal	COOH terminal	Nucleotide	Amino acid
All tumors						
Mean	0.28	0.29	28	27		
Median (range)	0.34 (0.00-0.55)	0.34 (0.00-0.55)	23 (0-75)	21 (0-66)		
Responders						
Mean	0.41	0.38	44	37		
Median (range)	0.43 (0.24-0.55)	0.36 (0.24-0.55)	48 (0-75)	36 (0-66)		
Nonresponders						
Mean	0.20	0.23	18	21		
Median (range)	0.26 (0.00-0.55)	0.30 (0.00-0.55)	5 (0-75)	17 (0-66)		
P§	<0.001	<0.001	<0.001	0.001		
Negative for COOH-terminal immunostaining and radioligand binding						
NR4	0.32	0.00	45	0	—	—
NR6	0.35	0.00	15	0	—	—
NR7	0.30	0.00	5	0	—	—
NR14	0.41	0.00	12	0	—	—
NR15	0.36	0.00	25	0	CAG-CAA	Gln-Gln^{858}
NR18	0.34	0.00	24	0	ATG-GTG	Met-Val^{807}
NR19	0.33	0.00	12	0	—	—
NR26	0.30	0.00	15	0	ATG-ACG	Met-Thr^{780}
NR33	0.52	0.00	65	0	—	—
Mean	0.36	0	24	0		
Median (range)	0.34 (0.30-0.52)	0 (0-0)	15 (5-65)	0 (0-0)		

*Mean absorbance (average intensity of AR immunoreactivity).
†Percent positive nuclear area (percentage of total nuclear area stained).
‡Numbering is per the *AR* gene mutations database (47).
§Mann-Whitney *U* test probability of difference from responders.

MPA (46.9 Ci/mmol; Amersham) for AR and stability of AR-ligand complexes were determined in cytosol extracts of COS-1 cells transfected with wtAR or AR variants as described previously (31, 32).

Molecular modeling. Models of MPA and DHT were constructed from molecular sketches drawn in ISIS draw 2.2.1[4] and converted to a three-dimensional representation in Sculpt 3.2. Partial charges and initial energy minimization of ligands were assigned in Vega 1.6.1 (33). The crystallographic structure of the AR LBD (34) was used to generate a model for docking. Water molecules and bound ligand in the structure file were deleted, hydrogen atoms were fixed to polar atoms, and the receptor was placed in a grid (100 × 100 × 100 units) with a spacing of 0.375 Å centered on the ligand-binding cavity. Ligands were docked into the LBD using Autodock 3.0 (35). The steroid nucleus of the ligands was left rigid, whereas the other bonds were allowed to rotate freely during docking simulation. The highest ranking solutions from both MPA and DHT docking simulations were reconfigured in SPDBV 3.7 such that hydrogens were reattached to polar atoms. *In silico* receptor mutation was done followed by energy minimization (200 steps of steepest descent with a 10 Å cutoff for nonbonded interactions). Ten independent 100ps molecular dynamic simulations for wild-type or mutant receptors bound to DHT or MPA were carried out allowing atoms within 15 Å of bound ligand to move under constant temperature conditions (300 K bath temperature, 1 fs step time, and 20 equilibration steps). The sets of 10 solutions for each receptor/ligand combination were superimposed using the entire receptor LBD as a reference point. Root mean square (RMS) deviation for side chains within 7 Å was calculated within SPDBV 3.7. Molecular surfaces were constructed using the GRASP implementation within SPDBV and figures were rendered using PovRay.[5]

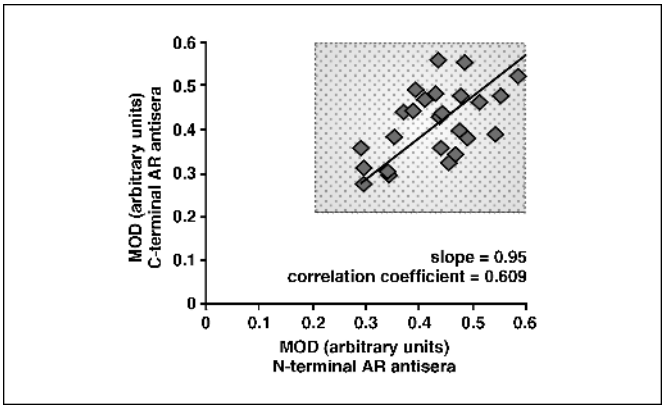

Figure 2. AR immunoreactivity in human prostate tumors. Comparison of the mean absorbance with NH_2- and COOH-terminal AR antisera in 26 primary human prostate tumors. Data for each antibody were generated using quantitative VIA of at least 20 fields of view chosen at random in each sample. The concordance between immunoreactivity detected with the NH_2- and COOH-terminal AR antisera is indicated along with the slope from a line of best fit for the data set. *Dotted box,* extent of positive immunoreactivity detected by both AR antisera in a subset of breast cancer samples.

[4] http://www.mdli.com/.
[5] http://www.povray.org.

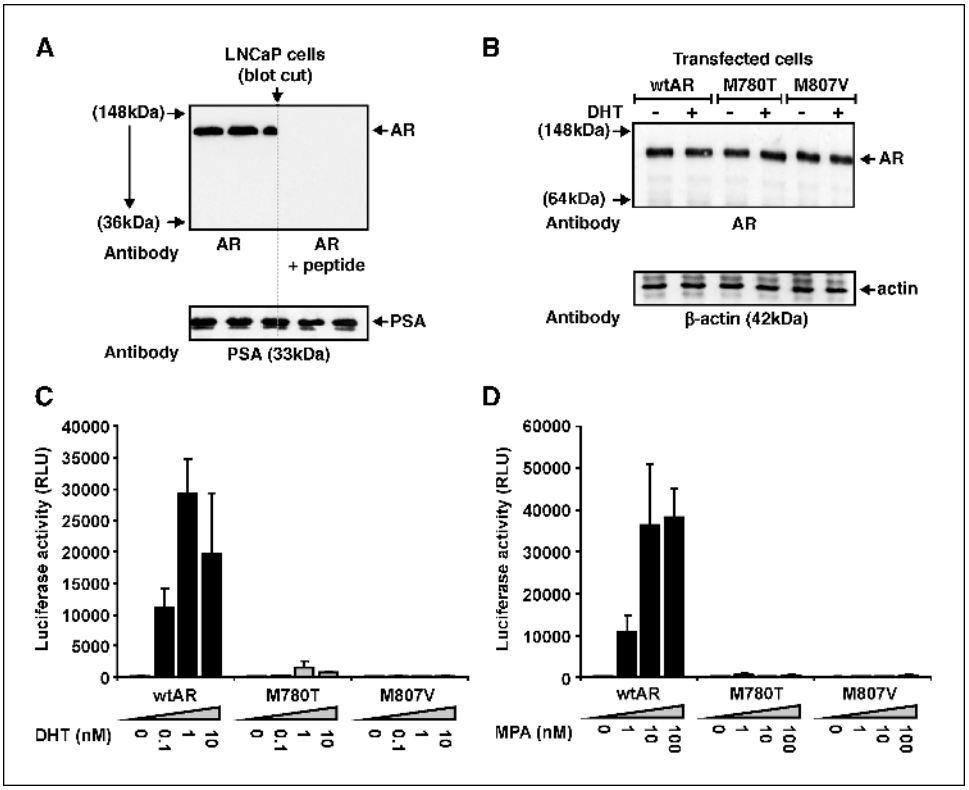

Figure 3. Analysis of level and transactivation capacity of wtAR and AR variants identified in clinical breast cancer samples. *A,* immunoblot detection of endogenous AR in lysates from LNCaP cells using the anti–NH_2-terminal AR antisera. Specificity of AR immunoreactivity is shown by blotting with the NH_2-terminal antibody after preincubation with a 5× excess by weight of the specific peptide. The androgen-responsive PSA protein was used as a loading control. *B,* immunoblot detection of AR and β-actin in lysates of COS-1 cells transfected with wtAR or AR variant expression vectors and treated with or without 1 nmol/L DHT as indicated. *C,* transactivation analysis of wtAR or AR variants in response to DHT (0-10 nmol/L as indicated) in transiently transfected MDA-MB-231 cells on the ARR3tk-luc (probasin) reporter gene. Luciferase activity is presented as relative light units and represents the mean ± SE of six to eight independently transfected wells. *D,* transactivation analysis of wtAR or AR variants in response to MPA. Assay was done with MPA (0-100 nmol/L) as detailed in (*C*).

Statistical analysis. Statistical analysis was done using the Statistical Package for the Social Sciences version 11.0 (SPSS, Chicago, IL). The Spearman's correlation and Mann-Whitney tests were used to compare AR immunostaining measurements with the two AR antibodies. The one-way ANOVA test and the Dunnet *post hoc* test were used to determine statistical significance between control and treatment groups. Statistical significance was set at $P < 0.05$.

Results

Androgen receptor immunostaining and response to medroxyprogesterone acetate therapy. To investigate further the potential role of AR in mediating response to MPA therapy in breast cancer, we conducted immunohistochemistry with two previously characterized antisera specific for the AR NH_2- and COOH-termini, respectively (26, 28), on serial paraffin sections of 83 tumor specimens of patients treated with MPA following failure of tamoxifen. Whereas the majority (48 of 83) of breast tumors in this cohort exhibited nuclear AR immunoreactivity with both NH_2- and COOH-terminal antisera (Fig. 1*A*), a small proportion (7 of 83) did not exhibit staining with either antibody, and approximately one-third (28 of 83) exhibited staining with only one or other of the two AR antisera (Fig. 1*A*; see example in Fig. 1*B*). Strong positive nuclear AR immunoreactivity with both NH_2- and COOH-terminal antisera was detected in all 32 samples from responders to MPA (Fig. 1*C*), of which 29 of 32 also showed AR radioligand binding. In contrast, tumors from nonresponders exhibited one of four distinct patterns of AR immunoreactivity: (*a*) strong staining with both antisera (16 of 51; 31%); (*b*) staining only with the COOH-terminal antibody (17 of 51; 33%); (*c*) staining only with the NH_2-terminal antibody (11 of 51; 22%); or (*d*) no immunoreactivity with either NH_2- or COOH-terminal antisera (7 of 51; 14%; Fig. 1*D*). For both antibodies, the mean intensity of AR immunoreactivity and the total proportion of nuclear area stained for AR were significantly less in nonresponders than in responders ($P < 0.001$; Table 1). AR immunoreactivity in nonresponders was also concordant with AR radioligand binding. Of the 16 of 51 samples positive for both AR antisera, 15 were positive for AR radioligand binding. Similarly, of the 17 of 52 nonresponders negative by radioligand binding, 15 were negative for AR immunostaining ($\chi^2 = 7.7$; $P = 0.02$).

To show that the greater heterogeneity of AR immunostaining with the two antisera in nonresponders to MPA reflects the AR status in those tumors rather than differences in the sensitivity of the AR NH_2- and COOH-terminal antisera, we similarly assessed AR immunoreactivity in a cohort of 26 untreated prostate tumors (Fig. 2). All 26 prostate tumor samples exhibited nuclear immunoreactivity with both NH_2- and COOH-terminal AR antisera, with a pattern of immunostaining similar to that for breast cancers that responded to MPA but distinct from nonresponders (Fig. 2). There

Table 2. Ligand binding affinity of DHT and MPA for the AR in transiently transfected COS-1 cells

	Median (SE) K_d (nmol/L)	
	DHT	MPA
wtAR	0.41 (0.07), $n = 12$*	0.72 (0.21), $n = 8$
AR-M780T	1.54 (0.41), $n = 3$	0.58 (0.16), $n = 3$
AR-M807V	No binding, $n = 5$	0.53 (0.15), $n = 5$

*n = number of independent assays.

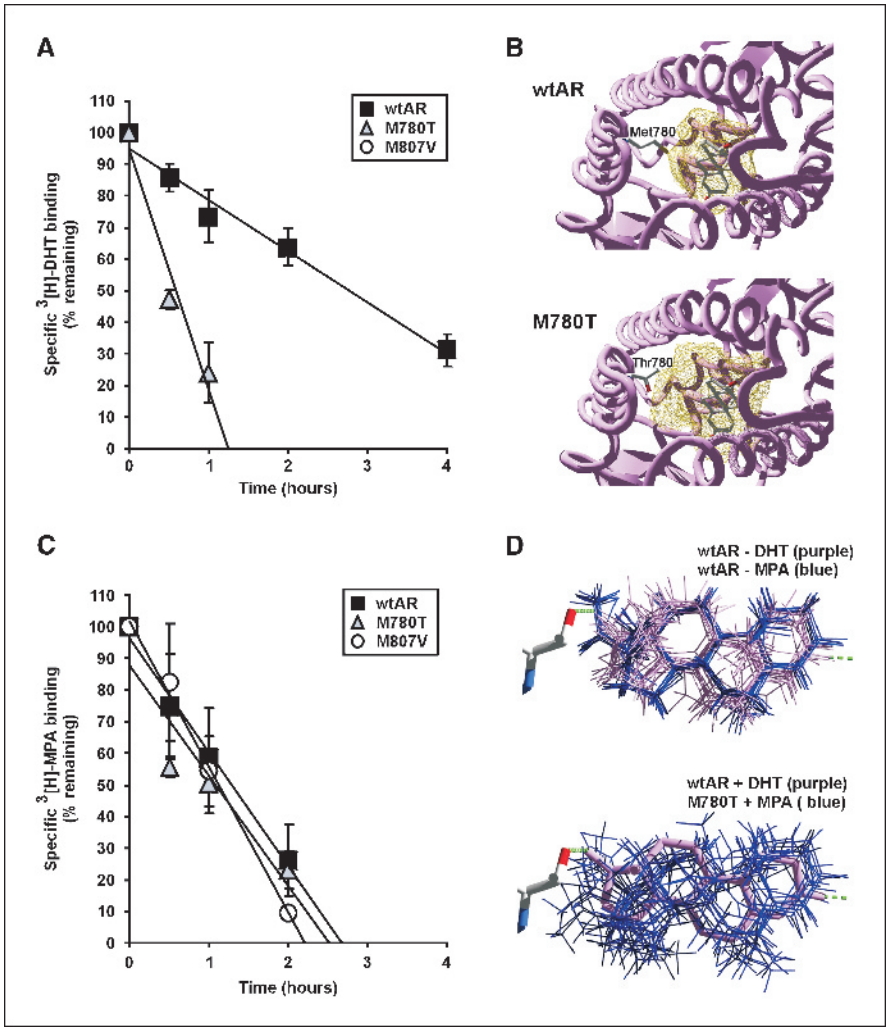

Figure 4. Stability of AR-ligand complexes and molecular modeling of wild-type and mutant AR. *A,* stability of receptor-DHT complexes done in cytosol fractions of COS-1 cells transfected with wtAR and AR variant expression vectors using DHT (126 Ci/mmol). *B,* comparison of the crystal structure of the wtAR ligand-binding pocket with that of AR-M780T generated using molecular modeling. The inner surface of the pocket is shown as a gold mesh. DHT and the Met^{780} residue are depicted in stick form and colored according to CPK convention. Substitution of Met^{780} by threonine causes a marked expansion of the ligand-binding pocket. *C,* stability of receptor-MPA complexes done in lysates of COS-1 cells transfected with wtAR and AR variant expression vectors using MPA (46.9 Ci/mmol). *D,* molecular dynamic simulation of ligand disposition in wtAR and AR-M780T. Ten independent molecular dynamic simulations of DHT (*purple*) and MPA (*blue*) binding to wtAR. The end points of each simulation were superimposed by fitting the LBD protein backbone onto the original crystal structure. The hydrogen bonds (*green*) associated to DHT with Arg^{754} and Thr^{877} are included as points of reference. There is little displacement of either DHT or MPA from the starting point of DHT in the crystal structure. In contrast, the model suggests that there is considerable disorder of MPA interaction with AR-M780T (*blue*) compared with DHT in the wtAR crystal structure (*purple*).

was a linear relationship between immunoreactivity determined with the NH_2- and COOH-terminal antisera in the prostate cancer samples (slope = 0.95; correlation coefficient = 0.609), indicating a high degree of concordance in the capacity to detect AR with the two antisera.

Detection of loss of function androgen receptor mutations in breast cancer samples. A subgroup of nine tumor samples from nonresponders exhibiting immunoreactivity with the NH_2-terminal AR antibody, but neither discernible AR radioligand binding nor immunostaining with the COOH-terminal AR antibody (Table 1), were analyzed for mutations in the *AR* gene. SSCP analysis and DNA sequencing of the coding region for the AR LBD (residues 670-919) identified mutations (two missense and one silent) in three of the tumor samples (Table 1). Using the NH_2-terminal AR antisera, we were able to specifically detect both endogenous AR (Fig. 3*A*) and ectopic wild-type and variant AR containing missense mutations (i.e., AR-M780T and AR-M807V) following transient transfection of AR-negative cell lines (Fig. 3*B*). Compared with wtAR, AR-M780T and AR-M807V were unable to activate the AR-responsive probasin promoter in transiently transfected MDA-MB-231 human breast cancer cells in the presence of either DHT or MPA (Fig. 3*B* and *C*). Similar results were obtained with the MMTV promoter in MDA-MB-231 cells and with both MMTV and probasin promoters in human prostate cancer (PC-3) and monkey kidney (COS-1) cells (data not shown).

Molecular basis for loss of medroxyprogesterone acetate function on androgen receptor variants detected in breast cancer. We initially investigated the basis of the defective response of AR-M780T and AR-M807V to DHT and MPA using ligand-binding analysis in transfected COS-1 cells and *in silico* modeling. The median $\pm$ SE of high-affinity binding sites for DHT and MPA in transfected cells was comparable, being 128 $\pm$ 32 and 112 $\pm$ 16 fmol/mg protein, respectively. This is consistent with our previous observation of comparable binding for MPA and DHT to the endogenous AR in the AR-positive, PR-negative human breast cancer cell line MDA-MB-453 (21). The AR-M780T variant had a moderately reduced relative binding affinity for DHT (Table 2) but exhibited a more markedly reduced stability compared with wtAR (Fig. 4*A*). AR-M807V had no apparent capacity to bind DHT (Table 2; Fig. 4*A*). *In silico* modeling of the AR-LBD determined that the methionine residue at position 780 forms a substantial part of the AR ligand-binding pocket, packing closely with the D-ring of bound DHT (Fig. 4*B*). Substitution of threonine for methionine at position 780 resulted in an increase in the volume of the ligand-binding pocket from 478 to 747 Å^3 (Fig. 4*B*), which may in part explain the lower binding affinity of the variant for DHT compared with wtAR.

In contrast to the results for DHT, the binding affinity of MPA for AR-M780T and AR-M807V was not significantly different to wtAR

(Table 2), and there was no difference in the stability of the AR-MPA complex for the variant receptors compared with wtAR (Fig. 4*C*). Analysis of the interaction between MPA and the wtAR by *in silico* docking analysis generated a binding solution that exhibited only a very small deviation (RMS of <0.1 Å) from the published crystal configuration of the DHT-bound receptor (ref. 34; Fig. 4*D*). In contrast, the predicted positioning of MPA in AR-M780T (Fig. 4*D*) and AR-M807V (data not shown) was highly variable, suggesting that both of these mutations have a destabilizing effect on receptor configuration in the presence of MPA.

Inverse relationship between progesterone receptor and androgen receptor in breast cancer cells. Although a significantly higher median AR level was determined by radioligand binding in the primary tumors of responders to MPA therapy compared with nonresponders, a similar level of ER was detected in both groups (Table 3*A*). Considering that the PR is a well-characterized *ER* target gene, it was surprising that there was a 3-fold higher median level of PR in nonresponders compared with responders, although this was not statistically significant (Table 3*A*). To investigate a potential relationship between AR and PR expression, we separated the cohort by median AR level (37 fmol/mg protein). Tumors with high AR had significantly lower median levels of PR (30 fmol/mg protein) compared with tumors with equal or lower than median AR (PR of 127 fmol/mg protein; $P < 0.05$; Table 3*B*). Considering that there was no difference in the level of ER between these two groups (Table 3*B*), these data suggest that the AR may act as a negative regulator of ER function in breast cancer cells.

Inhibition of estrogen receptor signaling by androgen receptor. We analyzed the effect of DHT and MPA on the estradiol-dependent proliferation of the AR-, ER-, and PR-positive T47D human breast cancer cell line. Increasing concentrations of DHT and MPA resulted in a significant ($P < 0.01$) dose-dependent decrease in T47D cell proliferation (Fig. 5*A* and *B*), reaching an inhibition ~50% of that achieved with 1 μmol/L of the ER antagonist, tamoxifen (Fig. 5*A*). DHT and MPA were also effective in inhibiting the estradiol-dependent growth of MCF-7 breast cancer cells (Fig. 5*C*), which are strongly positive for ER and AR but have very low levels of PR (insets in Fig. 5*B* and *C*). The inhibition of MCF-7 cell growth by DHT and MPA was reversed by treatment with a specific AR antisense oligonucleotide compared with the scrambled control (Fig. 5*C*). We confirmed for this experiment, as shown previously (2), a >50% reduction in the level of endogenous AR in cells treated with the AR antisense oligonucleotide compared with the scrambled oligonucleotide control (Fig. 5*C*). Consistent with an effect of AR on ER function, treatment of T47D cells with 10 nmol/L DHT resulted in an ~40% reduction in the capacity of estradiol to induce PR (Fig. 5*D*). These results are concordant with our analysis of PR mRNA in T47D cells by quantitative real-time PCR, where 10 nmol/L DHT or MPA reduced estradiol (1 nmol/L) induction of PR RNA levels by 71% and 83%, respectively. To determine if the AR exerts a direct inhibitory effect on ER function, as implied by the above experiments, we assessed ER activity in T47D cells transfected with an ER-specific reporter gene. DHT and MPA were able to inhibit ER activity induced by 1 nmol/L estradiol by >50% (Fig. 6*A*). In the steroid receptor-negative MDA-MB-231 human breast cancer cell line transfected with AR and ER expression vectors, increasing the ratio of AR to ER resulted in a dose-dependent increase in the inhibition of ER activity in the presence, but not the absence, of 1 nmol/L DHT (Fig. 6*B*).

Discussion

Although MPA has not been used extensively in the management of breast cancer since the advent of tamoxifen and aromatase inhibitors (13), there is considerable interest in its mode of action

Table 3.

A. Steroid receptor levels in breast tumors as determined by radioligand binding

Receptor	Median (range) radioligand binding (fmol/mg protein)		*P**
	Responders†	Nonresponders‡	
AR	107 (0-547)	15 (0-186)	<0.001
ER	91 (0-552)	78 (0-1,275)	0.885
PR	36 (0-893)	118 (0-2,322)	0.233

B. ER and PR levels in breast tumors by high or low AR protein

Receptor	Median (range) radioligand binding (fmol/mg protein)		*P*§
	Low AR‖ (≤37 fmol/mg protein)	High AR¶ (>37 fmol/mg protein)	
ER	82 (0-1,275)	79 (0-552)	0.767
PR	127 (0-2,221)	30 (0-2,322)	0.048

*Two-tailed probability, Mann-Whitney *U* test.
†Responders to MPA therapy ($n = 31$).
‡Nonresponders to MPA therapy ($n = 52$).
§Two-tailed probability, Mann-Whitney *U* test.
‖Tumors with ≤ median AR level ($n = 43$).
¶Tumors with > median AR level ($n = 40$).

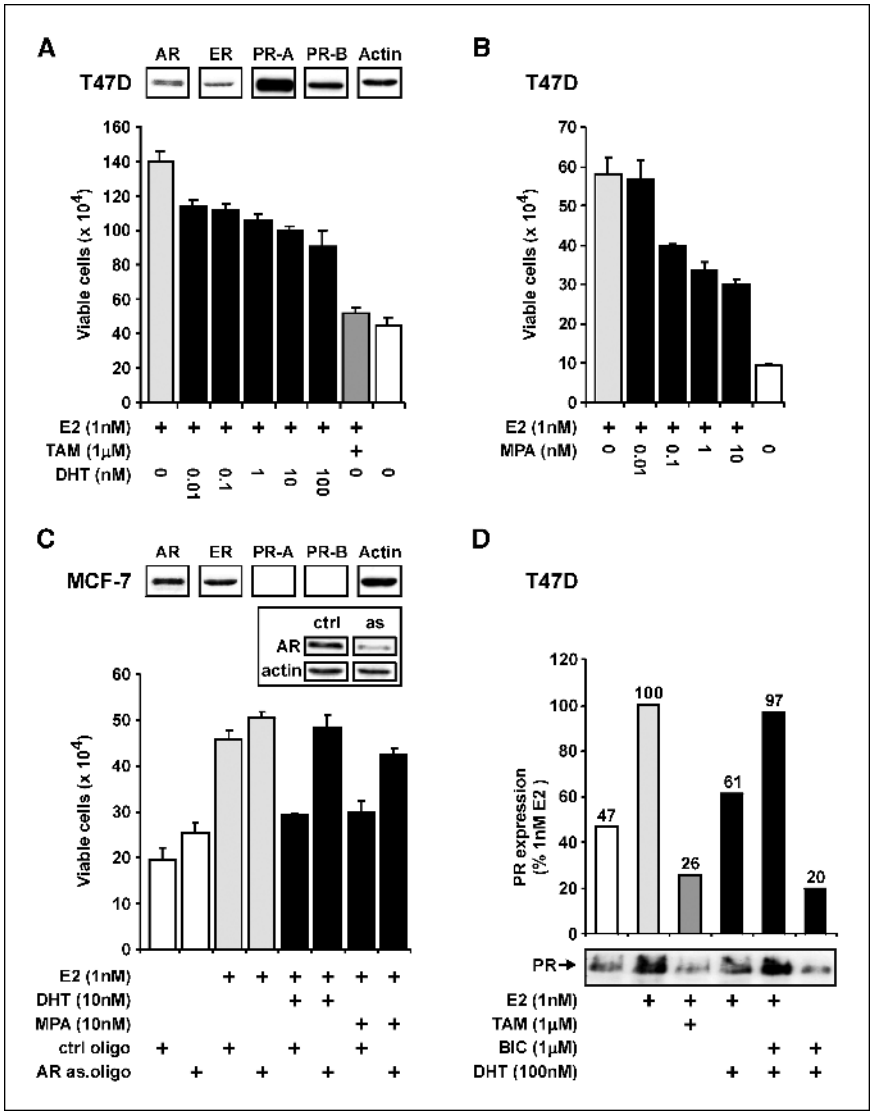

Figure 5. Inhibition of estrogen signaling in human breast cancer cells. *A,* effect of DHT on estradiol stimulated growth of human breast cancer T47D cells. Cells were treated as indicated with estradiol (*E2*) in the presence or absence of and/or the ER antagonist tamoxifen (*TAM*) or increasing concentrations of DHT or vehicle control. Viable cells were counted 9 days after initiation of treatment using a hemocytometer. Immunoblot analyses for AR, ER, PR-A, PR-B, and β-actin in untreated T47D cells are shown. *B,* effect of MPA on estradiol stimulated growth of T47D cells done as detailed in (*A*). *C,* effect of DHT and MPA on estradiol stimulated growth of MCF-7 human breast cancer cells. The level of AR, ER, PR-A, PR-B, and β-actin proteins in untreated MCF-7 cells are shown (same immunoblot and exposure as for T47D cells in *A*). Cells were transfected with AR antisense (*as*) oligonucleotide or a scrambled control (*ctrl*) and treated with ligands as indicated. Viable cells were counted 6 days after initiation of treatment using a hemocytometer. *Inset,* AR knockdown by antisense oligonucleotide compared with β-actin in this experiment. *D,* representative immunoblot analysis of PR in lysates from T47D cells treated as indicated with estradiol in the presence or absence of DHT and BIC for 48 hours. Quantification of immunoblot is presented as the percentage PR in the presence of 1 nmol/L estradiol.

given the results of the Woman's Health Initiative and the Million Women Study, among others, which document an increased risk of breast cancer in women taking MPA in the context of combined hormone replacement therapy (36, 37). We reported previously that response of breast tumors to the synthetic progestin, MPA, is dependent on the level of AR measured biochemically by radioligand binding in the primary tumors but not on PR status (23). However, the conundrum raised by that study was detection of AR in a significant proportion of nonresponders. In the present study, we provide evidence that both the level of the AR and its structure and/or function are critical for response to MPA. The loss of AR, implied by a lack of specific radioligand binding and immunoreactivity with antisera specific for the NH_2 and COOH termini of the receptor, most likely accounts for the lack of MPA response in a proportion of nonresponders. Strikingly however, >50% of the nonresponders to MPA exhibited strong immunoreactivity with one or other of the two AR antisera. Where immunoreactivity was detected with one or other antisera, the proportion of positive cells and the intensity of immunostaining were comparable with that observed in samples positive with both antisera, suggesting that altered AR structure or function, rather than loss of AR, may be responsible for the failure of response to MPA. Evidence supporting this hypothesis at a structural level was provided by the identification of missense *AR* gene mutations (i.e., M780T and M807V) in the LBD that prevent activation of the receptor by DHT and MPA. The mutations were identified by focusing on nine tumors that failed to respond to MPA and exhibited positive AR immunoreactivity with the NH_2-terminal antibody but negative with the COOH-terminal antisera and lacked specific DHT binding. These findings are consistent with clinical observations of the inherited syndrome of androgen insensitivity, where substitutions at codons 780 and 807 of the AR confer loss of function and result in the complete form of the disease (38).

Importantly, our results suggest that the lack of radioligand binding and AR immunostaining does not necessarily reflect either a loss of AR protein or an androgen insensitivity confering mutation in the LBD of the receptor. It is possible that structural changes or mutations elsewhere in the receptor, such as the AR NH_2 terminus or DNA-binding domain, could exert an effect on ligand binding and *in vivo* immunoreactivity with either NH_2- or COOH-terminal antisera. For example, assembly of the Hsp90 chaperone heterocomplex on the AR, which is intricately related to the capacity of steroid receptors to interact with their cognate ligands and to undergo cytoplasmic-nuclear translocation (39), involves specific motifs in the AR-NTD (40). Analogous to variation in the two

NH_2-terminal LxxLL-like peptides of the AR that interact with the LBD following ligand binding, mutations in regions required for heterocomplex formation could result in a faster dissociation rate of bound ligand from the receptor (41) or change LBD structure *in vivo*. Moreover, it was recently found that human tumor cells frequently evolve a more sensitized Hsp90 chaperone heterocomplex than present in normal epithelial cells (42). This provides a mechanism through which tumor-specific changes in chaperone expression, as has been observed in breast cancer (43, 44), could alter the conformation of the wild-type apo-AR and its capacity to bind ligand. Alternatively, as the COOH-terminal AR antibody is targeted to a region of the receptor known to form an integral part of the ligand and cofactor binding surface and to undergo significant ligand-dependent conformational change (34, 45), reduced immunoreactivity may occur in tumors where the levels of available ligand or specific cofactors are altered. Indeed, we have shown previously that the COOH-terminal AR antisera has a reduced ability to detect AR in the absence of DHT (28). For the group of tumors that failed to respond to MPA and were positive for the COOH-terminal AR antisera but negative for the NH_2-terminal antibody, changes in the length of the polyglutamine repeat in the receptor or predominant expression of the NH_2-terminal truncated isoform (AR-A) in lieu of the full-length AR (10, 46) provide alternative explanations for altered function and immunoreactivity. These possibilities are particularly relevant in the context of the current study, as the ability of MPA to activate the AR is critically dependent on a precise receptor conformation, congruent with its atypical agonist activity in the absence of a N/C interaction (47). Subtle changes in AR structure, brought about by alterations in the maturation/chaperone heterocomplex, phosphorylation of the receptor, or interaction with specific cofactors, could prevent MPA activation, ultimately resulting in its failure to inhibit breast cancer cell growth. In effect, structural changes bought about by these mechanisms may have the capacity to switch MPA from an agonist to an antagonist of the AR. The results of our molecular modeling suggest that the two AR variants identified in this study (i.e., M780T, M807V) have a destabilizing effect on receptor configuration in the presence of MPA. This may be sufficient to eliminate their capacity to become activated by MPA despite continued ability to bind the ligand.

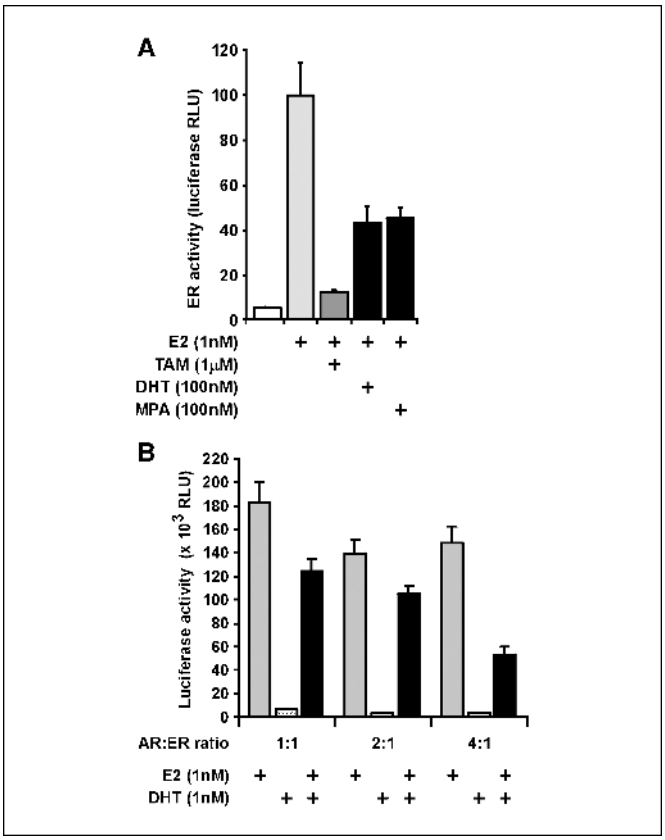

Figure 6. Inhibition of ER activity by AR. *A,* transactivation analysis of endogenous ER. Luciferase activity was determined in cell lysates 24 hours after transient transfection of T47D cells with the ER-specific reporter gene, ERE-tk-luc, and treatment with estradiol alone or in the presence of DHT, MPA, or TAM as indicated. Data are presented relative to the activity induced by 1 nmol/L estradiol and represents the mean ± SE of six independently transfected wells. *B,* effect of increasing AR levels on ER activity. ER-negative, AR-negative MDA-MB-231 breast cancer cells were transfected with ERE-tk-luc and with ER and AR expression vectors at a ratio of 1:1, 1:2, and 1:4 as indicated. Luciferase activity was determined in cell lysates 24 hours after treatment with estradiol and/or DHT. Data are presented as relative light units (*RLU*) and represent the mean ± SE of six independently transfected wells.

Identification in the entire breast cancer cohort of hormone-naive tumors of an inverse relationship between the level of AR and PR, despite similar levels of ER, suggested that AR may directly oppose ER-mediated growth of breast cancer cells. Our *in vivo* and *in vitro* data strongly support the hypothesis that the effects of androgens on breast cancer growth are mediated by specific activation of the AR rather than nonspecific effects on estrogen signaling. Importantly, increasing the amount of AR in breast cancer cell lines resulted in greater inhibition of ER function, which suggests that the level of AR in breast epithelial cells could influence estradiol-induced proliferation and the risk of developing cancer. Loss of AR activity or function in a breast tumor would thereby allow unopposed estrogen stimulation of PR expression and cell growth. A balance between estrogen and androgen signaling in the breast may help explain the epidemiologic data linking AR with breast cancer risk and breast density in women who take MPA as a component of HRT and the *in vivo* effects of androgens on mammary epithelial cell growth (9, 11, 14, 24, 48). Mechanistically, inhibition of ER could occur as a result of activation of AR-responsive gene pathways that negatively impact on ER function or by physical squelching of common coregulators recruited to the receptors following ligand binding (49). Alternatively, a physical interaction between the AR NH_2-terminal domain and the ER LBD, which causes a marked reduction in ER activity in yeast and mammalian cells (50), provides a direct mechanism for AR inhibition of ER signaling.

Our finding that immunohistochemistry with AR antisera to distinct epitopes detects discordant levels of AR in a subset of breast tumors, reflecting not only loss of AR protein but also alterations in AR structure, function, or signaling capacity, has important implications for the use of ER and PR immunostaining in the management of breast cancer. Utilization of a similar dual-antibody strategy for ER and PR could assist in the prediction of clinical responsiveness of breast tumors to conventional hormone therapy.

Acknowledgments

Received 8/25/2004; revised 7/2/2005; accepted 7/11/2005.

Grant support: National Health and Medical Research Council of Australia grant 250373 and U.S. Department of Defense grant W81XWH-04-1-0017.

The costs of publication of this article were defrayed in part by the payment of page charges. This article must therefore be hereby marked *advertisement* in accordance with 18 U.S.C. Section 1734 solely to indicate this fact.

We thank Dr. Christine Clarke for the PR antibody and Virginia Papangelis (Tissue Bank, Repatriation General Hospital, South Australia, Australia) for technical assistance and tissue sectioning, and Marie A. Pickering, Deborah Marrocco, and Kathleen M. Saint for technical assistance.

References

1. Scher HI, Buchanan G, Gerald W, Butler LM, Tilley WD. Targeting the androgen receptor: improving outcomes for castration-resistant prostate cancer. Endocr Relat Cancer 2004;11:459–76.
2. Birrell SN, Bentel JM, Hickey TE, et al. Androgens induce divergent proliferative responses in human breast cancer cell lines. J Steroid Biochem Mol Biol 1995;52:459–67.
3. Birrell SN, Hall RE, Tilley WD. Role of the androgen receptor in human breast cancer. J Mammary Gland Biol Neoplasia 1998;3:95–103.
4. Labrie F, Luu-The V, Labrie C, et al. Endocrine and intracrine sources of androgens in women: inhibition of breast cancer and other roles of androgens and their precursor dehydroepiandrosterone. Endocr Rev 2003; 24:152–82.
5. Somboonporn W, Davis SR. Testosterone effects on the breast: implications for testosterone therapy for women. Endocr Rev 2004;25:374–88.
6. Hall RE, Aspinall JO, Horsfall DJ, et al. Expression of the androgen receptor and an androgen-responsive protein, apolipoprotein D, in human breast cancer. Br J Cancer 1996;74:1175–80.
7. Kuenen-Boumeester V, Van Der Kwast TH, Claassen CC, et al. The clinical significance of androgen receptors in breast cancer and their relation to histological and cell biological parameters. Eur J Cancer 1996;32A:1560–5.
8. Pierre F, Bonnefoi H, Becette V, et al. Identification of molecular apocrine breast tumours by microarray analysis. Oncogene 2005;24:4660–71.
9. Haiman CA, Brown M, Hankinson SE, et al. The androgen receptor CAG repeat polymorphism and risk of breast cancer in the Nurses' Health Study. Cancer Res 2002;62:1045–9.
10. Buchanan G, Yang M, Cheong A, et al. Structural and functional consequences of glutamine tract variation in the androgen receptor. Hum Mol Genet 2004;13:1677–92.
11. Yu H, Bharaj B, Vassilikos EJ, Giai M, Diamandis EP. Shorter CAG repeat length in the androgen receptor gene is associated with more aggressive forms of breast cancer. Breast Cancer Res Treat 2000;59:153–61.
12. Tormey DC, Lippman ME, Edwards BK, Cassidy JG. Evaluation of tamoxifen doses with and without fluoxymesterone in advanced breast cancer. Ann Intern Med 1983;98:139–44.
13. Ingle JN, Twito DI, Schaid DJ, et al. Combination hormonal therapy with tamoxifen plus fluoxymesterone versus tamoxifen alone in postmenopausal women with metastatic breast cancer. An updated analysis. Cancer 1991;67:886–91.
14. Dimitrakakis C, Zhou J, Wang J, et al. A physiologic role for testosterone in limiting estrogenic stimulation of the breast. Menopause 2003;10:292–8.
15. Ortmann J, Prifti S, Bohlmann MK, Rehberger-Schneider S, Strowitzki T, Rabe T. Testosterone and 5α-dihydrotestosterone inhibit *in vitro* growth of human breast cancer cell lines. Gynecol Endocrinol 2002;16: 113–20.
16. Ando S, De Amicis F, Rago V, et al. Breast cancer: from estrogen to androgen receptor. Mol Cell Endocrinol 2002;193:121.
17. Parazzini F, Colli E, Scatigna M, Tozzi L. Treatment with tamoxifen and progestins for metastatic breast cancer in postmenopausal women: a quantitative review of published randomized clinical trials. Oncology 1993;50:483–9.
18. Zaucha R, Sosinska-Mielcarek K, Jassem J. Long-term survival of a patient with primarily chemo-resistant metastatic breast cancer treated with medroxyprogesterone acetate. Breast 2004;13:321–4.
19. Otani S, Toyota N, Nozaka K, et al. Successful combination therapy with 5′-DFUR and MPA for breast cancer with spinal and vertebral metastases. Gan To Kagaku Ryoho 2004;31:2151–3.
20. Focan C, Beauduin M, Majois F, et al. High-dose oral medroxyprogesterone acetate or tamoxifen as adjuvant hormone therapy for node-negative early-stage breast cancer: randomized trial with 7-year update. Clin Breast Cancer 2004;5:136–41.
21. Bentel JM, Birrell SN, Pickering MA, Holds DJ, Horsfall DJ, Tilley WD. Androgen receptor agonist activity of the synthetic progestin, medroxyprogesterone acetate, in human breast cancer cells. Mol Cell Endocrinol 1999;154:11–20.
22. Teulings FA, van Gilse HA, Henkelman MS, Portengen H, Alexieva-Figusch J. Estrogen, androgen, glucocorticoid, and progesterone receptors in progestin-induced regression of human breast cancer. Cancer Res 1980; 40:2557–61.
23. Birrell SN, Roder DM, Horsfall DJ, Bentel JM, Tilley WD. Medroxyprogesterone acetate therapy in advanced breast cancer: the predictive value of androgen receptor expression. J Clin Oncol 1995;13:1572–7.
24. Lillie EO, Bernstein L, Ingles SA, et al. Polymorphism in the androgen receptor and mammographic density in women taking and not taking estrogen and progestin therapy. Cancer Res 2004;64:1237–41.
25. Hackenberg R, Hawighorst T, Filmer A, Nia AH, Schulz KD. Medroxyprogesterone acetate inhibits the proliferation of estrogen- and progesterone-receptor negative MFM-223 human mammary cancer cells via the androgen receptor. Breast Cancer Res Treat 1993; 25:217–24.
26. Tilley WD, Lim-Tio SS, Horsfall DJ, Aspinall JO, Marshall VR, Skinner JM. Detection of discrete androgen receptor epitopes in prostate cancer by immunostaining: measurement by color video image analysis. Cancer Res 1994;54:4096–102.
27. Tilley WD, Buchanan G, Hickey TE, Bentel JM. Mutations in the androgen receptor gene are associated with progression of human prostate cancer to androgen independence. Clin Cancer Res 1996;2:277–85.
28. Husmann DA, Wilson CM, McPhaul MJ, Tilley WD, Wilson JD. Antipeptide antibodies to two distinct regions of the androgen receptor localize the receptor protein to the nuclei of target cells in the rat and human prostate. Endocrinology 1990;126: 2359–68.
29. Barnes WM. PCR amplification of up to 35-kb DNA with high fidelity and high yield from λ bacteriophage templates. Proc Natl Acad Sci U S A 1994;91:2216–20.
30. Buchanan G, Craft PS, Yang M, et al. PC-3 cells with enhanced androgen receptor signaling: a model for clonal selection in prostate cancer. Prostate 2004; 60:352–66.
31. Tilley WD, Marcelli M, Wilson JD, McPhaul MJ. Characterization and expression of a cDNA encoding the human androgen receptor. Proc Natl Acad Sci U S A 1989;86:327–31.
32. Grino PB, Isidro-Gutierrez RF, Griffin JE, Wilson JD. Androgen resistance associated with a qualitative abnormality of the androgen receptor and responsive to high dose androgen therapy. J Clin Endocrinol Metab 1989;68:578–84.
33. Pedretti A, Villa L, Vistoli G. VEGA: a versatile program to convert, handle and visualize molecular structure on Windows-based PCs. J Mol Graph Model 2002;21:47–9.
34. Sack JS, Kish KF, Wang C, et al. Crystallographic structures of the ligand-binding domains of the androgen receptor and its T877A mutant complexed with the natural agonist dihydrotestosterone. Proc Natl Acad Sci U S A 2001;98:4904–9.
35. Morris GM, Goodsell DS, Halliday RS, et al. Automated docking using a Lamarckian genetic algorithm and an empirical binding free energy function. J Comput Chem 1998;19:1639–62.
36. Beral V. Breast cancer and hormone-replacement therapy in the Million Women Study. Lancet 2003; 362:419–27.
37. Chlebowski RT, Hendrix SL, Langer RD, et al. Influence of estrogen plus progestin on breast cancer and mammography in healthy postmenopausal women: the Women's Health Initiative Randomized Trial. JAMA 2003;289:3243–53.
38. Gottlieb B, Beitel LK, Wu JH, Trifiro M. The androgen receptor gene mutations database (ARDB): 2004 update. Hum Mutat 2004;23:527–33.
39. Pratt WB, Toft DO. Steroid receptor interactions with heat shock protein and immunophilin chaperones. Endocr Rev 1997;18:306–60.
40. He B, Bai S, Hnat AT, et al. An androgen receptor NH_2-terminal conserved motif interacts with the COOH terminus of the Hsp70-interacting protein (CHIP). J Biol Chem 2004;279:30643–53.
41. He B, Kemppainen JA, Wilson EM. FXXLF and WXXLF sequences mediate the NH2-terminal interaction with the ligand binding domain of the androgen receptor. J Biol Chem 2000;275:22986–94.
42. Kamal A, Thao L, Sensintaffar J, et al. A high-affinity conformation of Hsp90 confers tumour selectivity on Hsp90 inhibitors. Nature 2003;425:407–10.
43. Thanner F, Sutterlin MW, Kapp M, et al. Heat-shock protein 70 as a prognostic marker in node-negative breast cancer. Anticancer Res 2003;23:1057–62.
44. Vargas-Roig LM, Fanelli MA, Lopez LA, et al. Heat shock proteins and cell proliferation in human breast cancer biopsy samples. Cancer Detect Prev 1997;21: 441–51.
45. Nettles KW, Greene GL. Ligand control of coregulator recruitment to nuclear receptors. Annu Rev Physiol 2005;67:309–33.
46. Gao T, McPhaul MJ. Functional activities of the A and B forms of the human androgen receptor in response to androgen receptor agonists and antagonists. Mol Endocrinol 1998;12:654–63.
47. Kemppainen JA, Langley E, Wong CI, Bobseine K, Kelce WR, Wilson EM. Distinguishing androgen receptor agonists and antagonists: distinct mechanisms of activation by medroxyprogesterone acetate and dihydrotestosterone. Mol Endocrinol 1999;13:440–54.
48. Liede A, Zhang W, Matsuda ML, Tan A, Narod SA. Androgen receptor gene polymorphism and breast cancer susceptibility in the Philippines. Cancer Epidemiol Biomarkers Prev 2003;12:848–52.
49. Hong H, Kohli K, Garabedian MJ, Stallcup MR. GRIP1, a transcriptional coactivator for the AF-2 transactivation domain of steroid, thyroid, retinoid, and vitamin D receptors. Mol Cell Biol 1997;17:2735–44.
50. Panet-Raymond V, Gottlieb B, Beitel LK, Pinsky L, Trifiro MA. Interactions between androgen and estrogen receptors and the effects on their transactivational properties. Mol Cell Endocrinol 2000;167:139–50.